

Universal Fractional Noncubic Power Law for Density of Metallic Glasses

Qiaoshi Zeng,^{1,2,4,5,*} Yoshio Kono,³ Yu Lin,¹ Zhidan Zeng,^{1,2,4,5} Junyue Wang,^{4,5} Stanislav V. Sinogeikin,³ Changyong Park,³ Yue Meng,³ Wenge Yang,^{4,5} Ho-Kwang Mao,^{4,5} and Wendy L. Mao^{1,2}

¹*Geological and Environmental Sciences, Stanford University, Stanford, California 94305, USA*

²*Photon Science and Stanford Institute for Materials and Energy Sciences,*

SLAC National Accelerator Laboratory, Menlo Park, California 94025, USA

³*HPCAT, Geophysical Laboratory, Carnegie Institution of Washington, 9700 South Cass Avenue, Argonne, Illinois 60439, USA*

⁴*HPSynC, Geophysical Laboratory, Carnegie Institution of Washington, 9700 South Cass Avenue, Argonne, Illinois 60439, USA*

⁵*Center for High Pressure Science and Technology Advanced Research (HPSTAR),*

1690 Cailun Road, Pudong, Shanghai 201203, People's Republic of China

(Received 21 March 2014; published 8 May 2014)

As a fundamental property of a material, density is controlled by the interatomic distances and the packing of microscopic constituents. The most prominent atomistic feature in a metallic glass (MG) that can be measured is its principal diffraction peak position (q_1) observable by x-ray, electron, or neutron diffraction, which is closely associated with the average interatomic distance in the first shell. Density (and volume) would naturally be expected to vary under compression in proportion to the cube of the one-dimensional interatomic distance. However, by using high pressure as a clean tuning parameter and high-resolution *in situ* techniques developed specifically for probing the density of amorphous materials, we surprisingly found that the density of a MG varies with the 5/2 power of q_1 , instead of the expected cubic relationship. Further studies of MGs of different compositions repeatedly produced the same fractional power law of 5/2 in all three MGs we investigated, suggesting a universal feature in MG.

DOI: 10.1103/PhysRevLett.112.185502

PACS numbers: 81.05.Kf, 61.05.cp, 62.50.-p

The macroscopic properties of materials are intimately linked to their microscopic structure. For crystals, their natural regular shapes (polyhedrons with faceted surfaces) reflect the strict atomic level packing symmetry in unit cells. Detailed unit cell information can be uncovered by diffraction techniques, which shows sharp Bragg peaks as a direct consequence of their long-range periodic arrangement of atoms. Microscopic length scale changes in a unit cell directly reflect its global three-dimensional (3D) density or volume change. In contrast, no such relationship has been established in glasses. Because of the lack of long-range translational periodicity, diffraction of glasses only yields a few broad peaks (haloes) rather than sharp Bragg peaks. Few constraints on the glass atomic packing have been discovered. A theoretical description of their atomic structure is very difficult and can only be done statistically since it requires a “unit cell” containing an infinitely large number of atoms. Thus, determining how the local atomic packing scales up to fill 3D space in glasses remains mysterious, which severely hinders our effort to establish the relationships connecting the microscopic atomic structure and the global properties of glasses [1–4]. Constraints from experiments are critical for the theoretical effort to resolve these problems.

Because of the removal of the constraints of charge neutrality and bond angles, metallic glasses (MGs) [5–7] are believed to have very dense and efficient packing of atoms and/or clusters [1,2,8]. In addition, no matter how different their pair distribution functions look in real space

(different specific atomic structure), their diffraction patterns in reciprocal space are usually quite similar, with a well-defined and symmetrical principal diffraction peak (PDP), typically located at $q_1 = 2$ to 3 \AA^{-1} ($2\pi/q_1$ falls into the range of the first neighbor atomic distance). While limited, this provides direct structural information at the atomic level and is expected to include the statistical information of average interatomic spacing (d) according to the well-known Ehrenfest relationship [9], i.e., $d \propto (1/q_1)$. The strong correlation between q_1 and d has been extensively observed [10–12] in MGs and was recently directly confirmed by a subnano beam transmission electron microscopy (TEM) study [13]. A cubic power law scaling, $V_a \propto (1/q_1)^D$, where the power D equals 3, and V_a is the average atomic volume, is expected for a macroscopic isotropic, disordered system. Based on these relationships, the easily measurable PDP position q_1 has been broadly employed to characterize the global strain [10,12] or density change [11,14] in various glasses. However, the nominally “disordered” glasses actually have been found to exhibit a very complex “ordered” atomic structure beyond short range order [1,2,15–20]. Thus, the use of those relationships for the complex glass structure is far from rigorous and thus has been controversial [4,21–24], which challenges the validity of many practical measurements and our basic understanding of glassy materials as well.

Pressure is a powerful and clean parameter which can simply increase the density (decrease the volume) of a MG

material over a large range. Having both accurate diffraction and density measurements for the compression of a MG would be the ideal way to clarify the power law relationship, in which V_a can be directly associated with the total volume V or reciprocal mass density $1/\rho$, because of the conservation of mass and number of atoms; thus, we have $V \propto (1/q_1)^D$ or $\rho \propto (q_1)^D$, and the mass density or volume change can be simply obtained,

$$\rho/\rho_0 = (q_1/q_{1_0})^D \text{ (or } V/V_0 = (q_{1_0}/q_1)^D), \quad (1)$$

where q_{1_0} is the initial PDP position. In the present study, we have experimentally determined the power D in the relationship (1) in MGs by combining the *in situ* high pressure x-ray diffraction (XRD), ultrasonic sound velocity measurements [25], and full field nanoscale x-ray transmission microscopy (TXM) [26].

In order to cover a large range of ρ and q_1 , we chose a very soft sample, $\text{La}_{62}\text{Al}_{14}\text{Cu}_{11.7}\text{Ag}_{2.3}\text{Ni}_5\text{Co}_5$ (L62) bulk metallic glass (BMG) [6,27] with small bulk modulus of ~ 41 GPa (details of the sample preparation are shown in the Supplemental Material [28]) to perform *in situ* high pressure XRD measurements (see Supplemental Material [28], Fig. S1). XRD patterns [Fig. 1(a)] on L62 BMG show no detectable crystallization or any phase transition with a smooth change of q_1 from 2.21 \AA^{-1} at 0.7 GPa to 2.50 \AA^{-1} at 22.8 GPa [Fig. 1(b)]. The q_1 returned to its initial position after pressure release (difference $< 0.1\%$), indicating completely elastic behavior during compression. To establish an accurate relationship between q_1 and ρ , independent measurement of density under high pressure is required.

How to accurately measure the density (volume) change of minute glass samples under high pressure has been a challenge for a long time [29]. Recent developments in ultrasonic sound velocity measurement using integrated ultrasonic interferometry, XRD, and x radiography in a large-volume high-pressure apparatus, e.g., a Paris-Edinburgh (PE) cell (Supplemental Material [28], Fig. S2), enables accurate compressional (P) and shear (S) wave velocity measurements as a function of pressure up to a few GPa on the L62 BMG sample [Fig. 2(a)] [25]. The density of L62 BMG as a function of pressure [Fig. 2(b)] can be calculated using the relationship between density, bulk modulus, and sound velocities (see Supplemental Material [28] for details). The density data can be fit very well by a third-order Birch-Murnaghan isothermal equation of state (BM-EOS) [30], with the isothermal bulk modulus $B_0 = 41.3 \pm 0.8 \text{ GPa}$ and its pressure derivative $B'_0 = 3.5 \pm 0.1$ [Fig. 2(b)], consistent with the reported value $B_0 \sim 41 \text{ GPa}$ for the L62 BMG [31]. Because of the relatively large sample size ($\sim 2 \text{ mm}$) required in ultrasonic experiments, the maximum pressure is limited. A direct measurement of the 3D volume to higher pressure would be valuable.

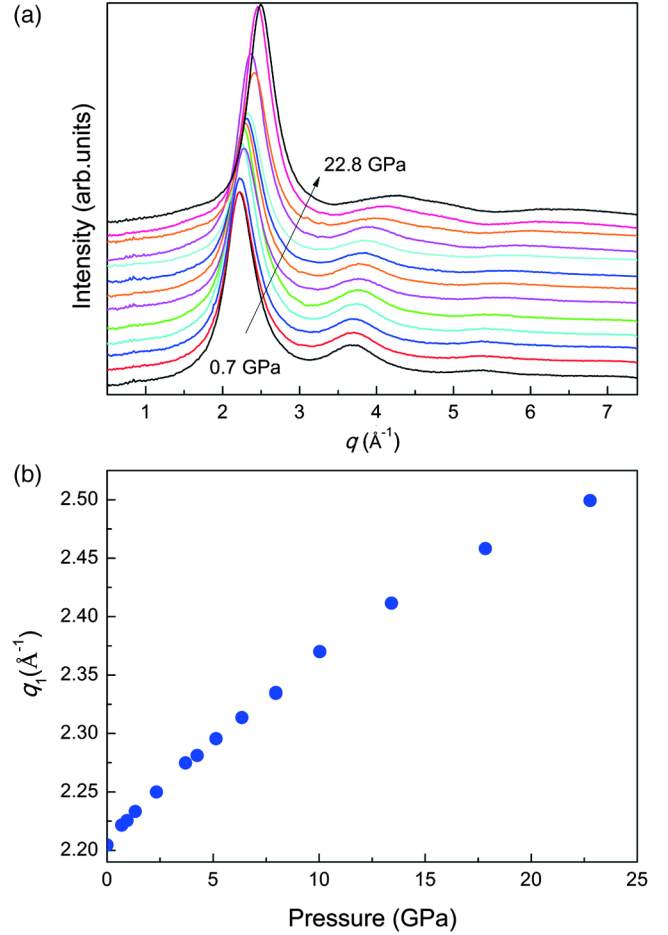


FIG. 1 (color online). *In situ* high pressure XRD measurements of L62 BMG. (a) XRD patterns with background subtracted from 0.7 to 22.8 GPa in a DAC. (b) Accurate principal diffraction peak positions (q_1) were fit by a Voigt line profile after subtracting the background, which shows a smooth shift as a function of pressure.

Recently, *in situ* high pressure nanoscale TXM in a diamond anvil cell (DAC) has been successfully developed, enabling the direct volume (or density) measurements of minute glass samples inside a DAC with high spatial resolution of 30 nm [26]. We performed TXM measurement (experimental details are shown in the Supplemental Material [28]) on the L62 BMG sample from 0.7 up to 20.5 GPa , using a newly developed cross DAC (see Supplemental Material [28], Fig. S4). The initial pressure was set at 0.7 GPa to keep the sample position stable in silicone oil (no movement during cell rotation). Figure 3(a) shows 3D renderings after reconstructing the 2D projection images at each pressure (see Supplemental Material [28], Fig. S5 for the 2D images, and Fig. S6 for 3D renderings at different viewing angles). The sample volume is proportional to the number of voxels within 3D segmentation. The density (or volume) change of the MG sample can thus be derived as shown in Fig. 3(b). The densities calculated from

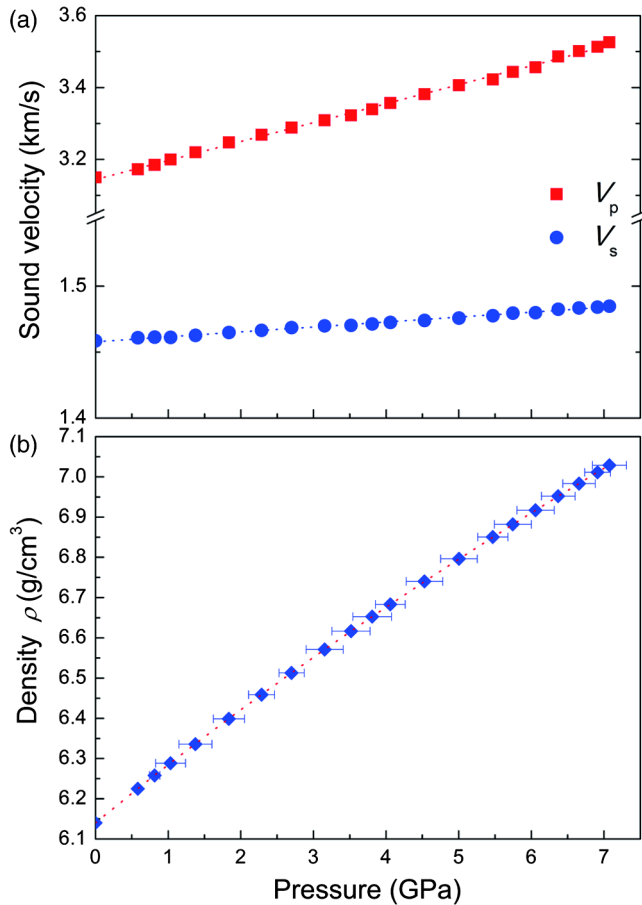


FIG. 2 (color online). Density measurement of L62 BMG using integrated ultrasonic sound velocity, x-ray radiography, and XRD measurements. (a) The sound velocities of the compression wave (V_p) and shear wave (V_s) as a function of pressure up to 7.1 GPa. (b) The density as a function of pressure obtained by calculation from ultrasonic sound velocities. The dotted line represents the fitting of density data using the third-order BM-EOS.

ultrasonic sound velocities and directly measured by TXM are highly consistent. We repeated the ultrasonic measurement on L62 BMG up to 5.3 GPa and confirmed the results were reproducible (Supplemental Material [28], Fig. S3).

Now that we have obtained both ρ (Fig. 3) and q_1 (Fig. 1) as a function of pressure, the relationship between ρ and q_1 can be simply established by transfer of variables. Figure 4 shows the density change (ρ/ρ_0) as a function of q_1/q_{10} for the L62 BMG sample. Indeed, the power law relation of $\rho/\rho_0 = (q_1/q_{10})^D$ is strictly followed over the entire range of compression. Surprisingly, however, all data points fit precisely the noncubic fractional power of $D = 5/2$, and obviously deviate from the expected cubic power of $D = 3$.

Is $D = 5/2$ a unique case that only applies for the L62 BMG? We further performed similar XRD and ultrasonic measurements on two additional BMGs. $\text{La}_{62}\text{Al}_{14}\text{Co}_{10.83}\text{Ni}_{10.83}\text{Ag}_{2.34}$ BMG was chosen for its very small initial PDP position q_{10} down to 2.18 \AA^{-1} , and

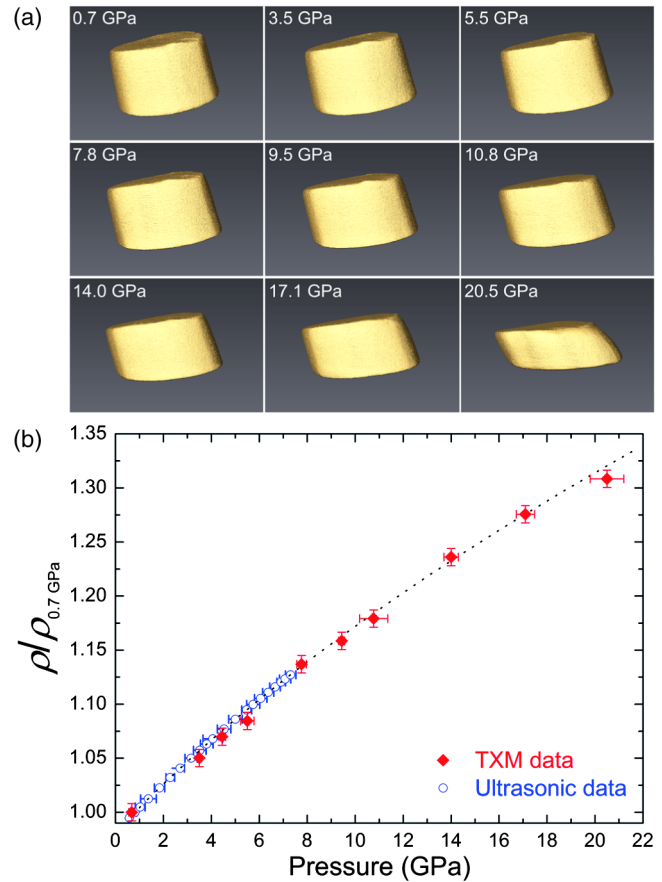


FIG. 3 (color online). Density measurement of L62 BMG using TXM. (a) 3D renderings iteratively reconstructed at different pressures. It is clear that the features in the initial rendering at 0.7 GPa are identical to those observed in the SEM image (see Supplemental Material [28], Fig. S4). (b) Density ($\rho/\rho_{0.7 \text{ GPa}}$) obtained by TXM (solid red diamonds) compared with density obtained by ultrasonic sound velocity calculation (open blue circles). The dotted line represents the fitting of density from ultrasonic measurement below 7.1 GPa using the third-order BM-EOS. The two density data sets collected using independent techniques are very consistent.

$\text{Cu}_{47}\text{Ti}_{33}\text{Zr}_{11}\text{Ni}_8\text{Nb}_1$ BMG for its q_{10} up to 2.86 \AA^{-1} , thus extending the range of q_1 almost to the limits of BMG (typically $2.1\text{--}2.9 \text{ \AA}^{-1}$). Surprisingly again, these two BMGs also closely fit the $D = 5/2$ fractional power law relationship (Fig. 4). Quantitative fitting of the relationship (1) for each sample yields $D = 2.51 \pm 0.05$ for L62 BMG, $D = 2.45 \pm 0.05$ for $\text{La}_{62}\text{Al}_{14}\text{Co}_{10.83}\text{Ni}_{10.83}\text{Ag}_{2.34}$ BMG and $D = 2.61 \pm 0.06$ for $\text{Cu}_{47}\text{Ti}_{33}\text{Zr}_{11}\text{Ni}_8\text{Nb}_1$ BMG. Close fitting of the noncubic $D = 5/2$ power to all three BMGs strongly suggests that the fractional $D = 5/2$ may be a universal characteristic of MGs.

Stimulated by both the scientific and practical significance of MGs, thousands of MGs with various compositions have been synthesized over the past decades. Thus, abundant diffraction and density data of MGs with various

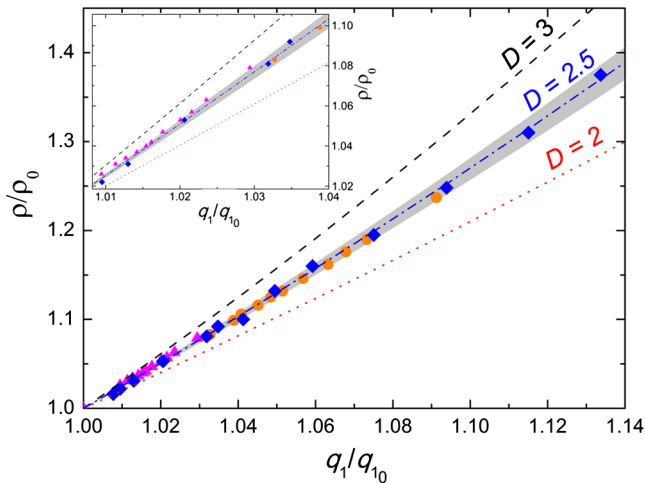


FIG. 4 (color online). The relative density change (ρ/ρ_0) as functions of the relative PDP position change (q_1/q_{10}) for three BMG samples: L62 (blue diamonds), $\text{La}_{62}\text{Al}_{14}\text{Co}_{10.83}\text{Ni}_{10.83}\text{Ag}_{2.34}$ (orange circles), and $\text{Cu}_{47}\text{Ti}_{33}\text{Zr}_{11}\text{Ni}_8\text{Nb}_1$ (magenta triangles). The lines represent the relationship $\rho/\rho_0 = (q_1/q_{10})^D$ to guide the eye with different D values: $D = 3$ (black dashed line), $D = 2.5$ (blue dash-dotted line), $D = 2$ (red dotted line). Three samples follow the $5/2$ power law very well. The gray zone represents the region with $D = 2.5 \pm 0.1$.

compositions are available. Using composition as a tuning variable, a 2.3 power law had been proposed [21], which is close to our finding of $D = 2.5$ with pressure tuning. The 2.3 compositional power law has been the subject of intense debate due to the complexity caused by compositional change [4,21–24], which involves many other variables, e.g., topological structure, scattering factors, chemical interaction, thermal history, etc. Thus the pressure employed in this work provides us a unique and clean means of tuning density in a straightforward way which enables us to clarify the intense controversy and provides compelling evidence of a universal fractional noncubic ($D = 5/2$) power law scaling of density for MGs. This noncubic power law relationship seems to contradict our common understanding of glass structure. It may be associated with the packing efficiency change as a function of the constituent atomic radii distribution in multi-component MG systems. However, due to our very limited knowledge about detailed atomic packing in MGs, the underlying origin cannot be resolved in the present work, which calls for further efforts combining simulations.

In summary, although the density (volume) of ordered crystals, disordered molecular gases [21], and even disordered liquids [22,23,32] usually follows an intuitive cubic power law of their PDP position q_1 , our results provide compelling evidence that the density of solid MGs follows an unexpected universal fractional noncubic ($5/2$) power law. This result is not just a refinement of the power value from 3 to $5/2$ which is critical for correcting and guiding the practical *in situ* measurements of density under

various environments (especially when the density changes a lot, the difference between the power of 3 and the power of $5/2$ will become significant) or any other measurements involving changes in length scale in MGs. More importantly, it rigorously establishes a relationship between the atomic scale structure information and the macroscopic scale property (density) in the “disordered” MG system, which resolves the controversy about the power law in MGs and provides a new critical constraint on glass structure modeling. The universal noncubic power law scaling of density, suggesting a common structural characteristic in MG systems, may bring new insight into the structural mechanism of good glass forming ability in multi-component MGs. Meanwhile, questions triggered by this work, such as, “What is the structural origin of the fractional $5/2$ power? Why is it so tightly constrained? Does it define the nature of MG? Is it valid in other glass systems as well?” will attract broad research interest leading to a deeper understanding of glasses and other disordered materials [33].

We thank Curtis Kenney-Benson, Yuxin (Steve) Wang, Sergey N. Tkachev, and Hongbo Lou for their great help with the experiments and Hongwei Sheng, Guoyin Shen, Wei Liu, and Yijin Liu for helpful discussions. This work is supported by DOE Office of Basic Energy Sciences, Materials Sciences and Engineering Division, under Contract No. DE-AC02-76SF00515. The XRD, ultrasonic and TXM experiments were performed at beamlines 16ID-B, 16BM-B and 32ID-C respectively at APS, ANL. Use of the HPCAT facility is supported by DOE-NNSA under Award No. DE-NA0001974 and DOE-BES under Award No. DE-FG02-99ER45775, with partial instrumentation funding by NSF. Use of the gas loading system at GSECARS was supported by NSF (EAR-0622171, EAR 06-49658 and EAR 10-43050), DOE (DE-FG02-94ER14466), and COMPRES. APS is supported by DOE-BES, under Contract No. DE-AC02-06CH11357. J. W. and W. Y. are supported by DOE-BES, under Contract No. DE-SC0001057.

*Corresponding author.

qzeng@carnegiescience.edu

- [1] D. B. Miracle, *Nat. Mater.* **3**, 697 (2004).
- [2] H. W. Sheng, W. K. Luo, F. M. Alamgir, J. M. Bai, and E. Ma, *Nature (London)* **439**, 419 (2006).
- [3] D. B. Miracle, T. Egami, K. M. Flores, and K. F. Kelton, *MRS Bull.* **32**, 629 (2007).
- [4] Y. Q. Cheng and E. Ma, *Prog. Mater. Sci.* **56**, 379 (2011).
- [5] A. L. Greer, *Science* **267**, 1947 (1995).
- [6] J. Schroers, *Phys. Today* **66**, No. 2, 32 (2013).
- [7] A. L. Greer and E. Ma, *MRS Bull.* **32**, 611 (2007).
- [8] J. D. Bernal, *Nature (London)* **185**, 68 (1960).
- [9] A. Guinier, *X-Ray Diffraction: In Crystals, Imperfect Crystals and Amorphous Bodies* (Dover, New York, 1994), p. 61.

- [10] H. F. Poulsen, *Nat. Mater.* **4**, 33 (2005).
- [11] A. R. Yavari, A. Le Moulec, A. Inoue, N. Nishiyama, N. Lupu, E. Matsubara, W. José Botta, G. Vaughan, M. Di Michiel, and Å. Kvik, *Acta Mater.* **53**, 1611 (2005).
- [12] T. C. Hufnagel, R. T. Ott, and J. Almer, *Phys. Rev. B* **73**, 064204 (2006).
- [13] A. Hirata, P. Guan, T. Fujita, Y. Hirotsu, A. Inoue, A. R. Yavari, T. Sakurai, and M. Chen, *Nat. Mater.* **10**, 28 (2011).
- [14] C. Meade, R. J. Hemley, and H. K. Mao, *Phys. Rev. Lett.* **69**, 1387 (1992).
- [15] Q. S. Zeng, H. Sheng, Y. Ding, L. Wang, W. Yang, J.-Z. Jiang, W. L. Mao, and H.-K. Mao, *Science* **332**, 1404 (2011).
- [16] S. R. Elliott, *Nature (London)* **354**, 445 (1991).
- [17] P. S. Salmon, R. A. Martin, P. E. Mason, and G. J. Cuello, *Nature (London)* **435**, 75 (2005).
- [18] A. Hirata, L. J. Kang, T. Fujita, B. Klumov, K. Matsue, M. Kotani, A. R. Yavari, and M. W. Chen, *Science* **341**, 376 (2013).
- [19] A. R. Yavari, *Nature (London)* **439**, 405 (2006).
- [20] Y. Q. Cheng, E. Ma, and H. W. Sheng, *Phys. Rev. Lett.* **102**, 245501 (2009).
- [21] D. Ma, A. D. Stoica, and X. L. Wang, *Nat. Mater.* **8**, 30 (2009).
- [22] P. Chirawatkul, A. Zeidler, P. S. Salmon, S. Takeda, Y. Kawakita, T. Usuki, and H. E. Fischer, *Phys. Rev. B* **83**, 014203 (2011).
- [23] O. F. Yagafarov, Y. Katayama, V. V. Brazhkin, A. G. Lyapin, and H. Saitoh, *Phys. Rev. B* **86**, 174103 (2012).
- [24] N. Mattern, M. Stoica, G. Vaughan, and J. Eckert, *Acta Mater.* **60**, 517 (2012).
- [25] Y. Kono, C. Park, T. Sakamaki, C. Kenny-Benson, G. Shen, and Y. Wang, *Rev. Sci. Instrum.* **83**, 033905 (2012).
- [26] J. Y. Wang, W. Yang, S. Wang, X. Xiao, F. De Carlo, Y. Liu, and W. L. Mao, *J. Appl. Phys.* **111**, 112626 (2012).
- [27] W. H. Wang, *Adv. Mater.* **21**, 4524 (2009).
- [28] See Supplemental Material at <http://link.aps.org/supplemental/10.1103/PhysRevLett.112.185502>, which includes Ref. [34–40].
- [29] H. Liu, L. Wang, X. Xiao, F. De Carlo, J. Feng, H.-k. Mao, and R. J. Hemley, *Proc. Natl. Acad. Sci. U.S.A.* **105**, 13 229 (2008).
- [30] F. Birch, *J. Geophys. Res.* **57**, 227 (1952).
- [31] Q. K. Jiang, G. Q. Zhang, L. Yang, X. D. Wang, K. Saksl, H. Franz, R. Wunderlich, H. Fecht, and J. Z. Jiang, *Acta Mater.* **55**, 4409 (2007).
- [32] N. W. Ashcroft and J. Lekner, *Phys. Rev.* **145**, 83 (1966).
- [33] C. Song, P. Wang, and H. A. Makse, *Nature (London)* **453**, 629 (2008).
- [34] H. K. Mao, J. Xu, and P. M. Bell, *J. Geophys. Res.* **91**, 4673 (1986).
- [35] P. Loubeyre, R. LeToullec, D. Hausermann, M. Hanfland, R. J. Hemley, H. K. Mao, and L. W. Finger, *Nature (London)* **383**, 702 (1996).
- [36] Y. R. Shen, R. S. Kumar, M. Pravica, and M. F. Nicol, *Rev. Sci. Instrum.* **75**, 4450 (2004).
- [37] O. L. Anderson, D. G. Isaak, and S. Yamamoto, *J. Appl. Phys.* **65**, 1534 (1989).
- [38] Y. Lin, Q. Zeng, W. Yang, and W. L. Mao, *Appl. Phys. Lett.* **103**, 261909 (2013).
- [39] Y. J. Liu, F. Meirer, P. A. Williams, J. Wang, J. C. Andrews, and P. Pianetta, *J. Synchrotron Radiat.* **19**, 281 (2012).
- [40] P. A. Yushkevich, J. Piven, H. Cody Hazlett, R. G. Smith, S. Ho, J. C. Gee, and G. Gerig, *NeuroImage* **31**, 1116 (2006).